Thermoeconomic Analysis of a Steam Rankine Cycle Integrated with Parabolic Trough Solar Collectors

Seyyed Masoud Seyyedi[1*]

Abstract – Solar energy is a renewable source that can be used for a wide range of applications especially for power generation. In this paper, thermoeconomic analysis is performed for a steam Rankine cycle whereas solar energy is used for producing steam using parabolic trough solar collectors (PTSC). For this purpose, firstly the modeling of the solar collectors is performed. Then the mass and energy equations are solved to obtain the thermodynamic state of each point. The cost of each component is calculated using the purchase costs of the system components as a function of thermodynamic parameters. The effect of active parameters such as inlet temperature and pressure of steam turbine, solar irradiation intensity, pinch point, interest rate, and lifetime are investigated on the number of solar collectors in rows, the total aperture area, the thermal efficiency and the average cost of electricity. The results shows that the average cost of electricity decreases with increasing the inlet temperature and pressure of steam turbine. The average cost of electricity is calculated to be less than 3 cent/kWh while it is normally more than 10 cent/kWh.

Keywords: Thermoeconomic, Cost of Electricity, Steam Turbine, Parabolic Solar Collector.

1. Introduction

Solar energy is a reliable energy source. It is a free renewable energy source with no gas emissions. Finding a more energy-efficient system with low cost of electricity is one of the most interested subjects in the design of energy systems. Solar energy can be used to obtain electrical power directly through photovoltaic solar cells or in directly through a solar thermal system. There are several solar thermal systems that can be used to produce electrical power through thermal power plants; these include Parabolic trough solar collectors(PTSC) , solar towers, and solar dishes. PTSC technology is considered the most established solar thermal technology for power production. Many researchers worked on the power generation using PTSC.

In 2006, Zarza et al. [1] investigated the conceptual design of a solar power plant using direct steam generation in a PTSC field. In 2010, Zheng and Weng [2] studied the performance of a cooling-cogeneration system for power and refrigeration production, using R245fa as a working fluid for the Rankine cycle. In 2011, energy performance assessment of a trigeneration system using PTSC and ORC was conducted by Al-Sulaiman et al [3]. In 2012, a detailed thermal model of a parabolic trough collector receiver was performed by Kalogirou [4]. Also, in 2012, Niknia et al. [5] carried out a simulation to examine the performance of a power plant integrated with PTSC and an auxiliary boiler. In 2013, energy and sizing analyses of parabolic trough solar collector integrated with steam and binary vapor cycles were performed by Al-Sulaiman et al [6]. Also, in 2014, he examined the exergy analysis of parabolic trough solar collectors integrated with combined steam and organic Rankine cycles[7]. In 2016, Nasir et al. [8] investigated the effect of working fluid on the performance of an ORC. In 2018, exergoeconomic analysis and optimization of a solar based multigeneration system using multiobjective differential evolution algorithm was performed by Rashidi et al. [9]. In 2019, Khanmohammadi et al.[10] performed thermodynamic and economic analyses for abiomass gasifier and thermoelectric generator. In 2019, in order to decrease the power consumption of cascade refrigeration cycle, a new combined cycle was proposed by Khalilzadeh et al. [11]. They used PTSC for this aim.

In this paper, thermoeconomic analysis is performed for

1* Corresponding Author :
Department of Mechanical Engineering, Aliabad Katoul Branch, Islamic Azad University, Aliabad Katoul ,Iran,
Email: s.masoud_seyedi@yahoo.com
Received:2020.12.18 ; Accepted: 2021.01.29

a steam Rankine cycle (SRC) whereas solar energy is used for producing steam using PTSC. The average cost of electricity is considered as objective function that must be minimized.

2. System descriptions

The considered system is a PTSC integrated with a SRC, as shown in Fig. 1. The system consists of a PTSC field, an evaporator, a steam turbine, a condenser, a solar pump, a steam pump and an electrical generator. The solar collector field consists of hundreds of solar collector rows. Each collector row consists of ten modules of collectors. The working fluid in the receiver pipe is Thermonil-VP1 since this oil has good heat transfer properties. Also, schematic of the parabolic trough solar collector is shown in Fig. 2. The geometric data of the solar collectors are given in Table 1.

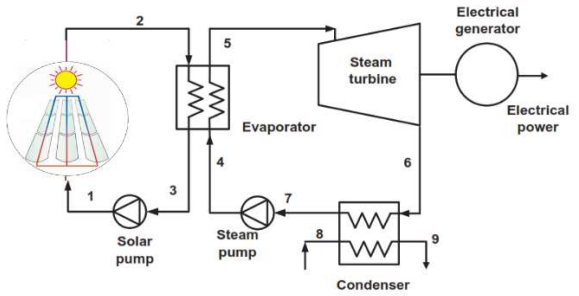

Fig.1 Schematic of the parabolic trough solar collectors integrated with steam Rankine cycle

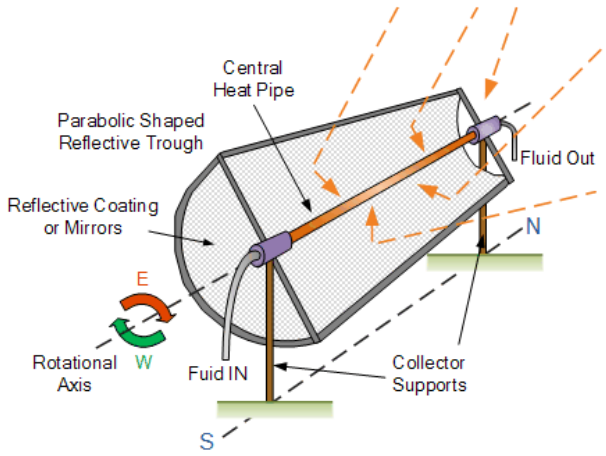

Fig.2 Schematic of the parabolic trough solar collector (PTSC)[12]

Table 1. Input values of the system

Name	Value	Name	Value
Single collector width	$W = 5.76$ m	Steam turbine efficiency	$\eta_{st} = 0.88$
Single collector length	$L = 12.27$m	Steam pump efficiency	$\eta_P = 0.85$
Receiver inner diameter	$D_{r,i} = 0.055$ m	Number of collectors in series	$Col_s = 10$
Receiver outer diameter	$D_{r,o} = 0.070$ m	Ambient temperature	$T_a = 10$ ℃
Cover inner diameter	$D_{c,i} = 0.125$ m	Ambient pressure	$P_a = 101.3$ kPa
Cover outer diameter	$D_{c,o} = 0.130$ m	Thermal conductivity of receiver pipe	$k_r = 16\ Wm^{-1}K^{-1}$
Emittance of the cover	$\varepsilon_c = 0.88$	Salvage percentage	$\mu = 15\%$
Emittance of the receiver	$\varepsilon_r = 0.31$	Working hour per year	$\tau = 7446$ hr
Reflectance of the mirror	$\rho_c = 0.94$	Maintenance factor	$\varphi = 1.06$
Intercept factor	$\gamma = 0.93$	Net electrical power	$\dot{W}_{net} = 20$ MW
Transmittance of the glass cover	$\tau_c = 0.96$		
Absorbance of the receiver	$\alpha_r = 0.96$		
Incidence angle modifier	$K_\gamma = 1$		

3. Mathematical modeling

Here, the mathematical modeling of the system is presented. The equations for the energy analysis of the PTSC, mass and energy balance equations for Rankine cycle and economic model equations are written.

3.1. Modeling of PTSC

The useful energy rate from the collector is defined as:

$$\dot{Q}_u = \dot{m}_r C_p (T_{fo} - T_{fi}) = \dot{m}_r (h_{fo} - h_{fi}) \quad (1)$$

On the other hand, it can be obtained by:

$$\dot{Q}_u = F_R\left(SA_{ap} - A_r U_L(T_{fi} - T_a)\right) \quad (2)$$

The heat removal factor $(F_R)$is defined as:

$$F_R = \frac{\dot{m}_r C_p}{A_r U_L}\left[1 - \exp\left(\frac{-A_r U_L F'}{\dot{m}_r C_p}\right)\right] \quad (3)$$

where

$$F' = \frac{U_O}{U_L} \quad (4)$$

and

$$U_O = \left[\frac{1}{U_L} + \frac{D_{r,o}}{h_f D_{r,i}} + \frac{D_{r,o}\ln(D_{r,o}/D_{r,i})}{2k_r}\right]^{-1} \quad (5)$$

In Eq. (2), the aperture area is defined as:

$$A_{ap} = (W - D_{c,o})L \quad (6)$$

The heat absorbed(S) bythe receiver is defined as:

$$S = G_b \eta_r \quad (7)$$

where,

$$\eta_r = \rho_c \tau \alpha \gamma K_\gamma \quad (8)$$

Heat loss from receiver to ambient can be calculated using Eqs.(9)-(12):

$$Q_{loss} = \frac{2\pi k_{eff} L}{\ln\left(\frac{D_{c,i}}{D_{r,o}}\right)}(T_{r,o} - T_{c,i}) + \frac{\pi\sigma D_{r,o} L}{\frac{1}{\varepsilon_r} + \frac{1-\varepsilon_c}{\varepsilon_c}\ln\left(\frac{D_{r,o}}{D_{c,i}}\right)}(T_{r,o}^4 - T_{c,i}^4) \quad (9)$$

$$Q_{loss} = \frac{2\pi k_c L}{\ln\left(\frac{D_{c,o}}{D_{c,i}}\right)}(T_{c,i} - T_{c,o}) \quad (10)$$

$$Q_{loss} = \pi D_{c,o} L h_w (T_{c,o} - T_a) + \pi L D_{c,o}\sigma\varepsilon_c(T_{c,o}^4 - T_{sky}^4) \quad (11)$$

$$Q_{loss} = A_r U_L(T_{r,o} - T_a) \quad (12)$$

In the Eq. (11), the outside convective heat transfer coefficient(h_w) can be calculated by:

$$Nu_w = h_w D_{c,o}/k_{air} \quad (13)$$

where,

$$Nu_w = \begin{cases} 0.4 + 0.54Re^{0.52} & \text{for } 0.1 < Re < 1000 \\ 0.3Re^{0.6} & \text{for } 1000 < Re < 50000 \end{cases} \quad (14)$$

Also, the convection heat transfer coefficient at the inside receiver, $(h_f)$is given by:

$$Nu_f = h_f D_{r,i}/k_f$$

where, the Nusselt number for laminar and turbulent flow regimes is obtained by Eqs. (15) and (16), respectively:

$$Nu_f = 4.36 \quad \text{for} Re_D < 2300 \quad (15)$$

$$Nu_f = \left[\frac{f}{8}(Re_D - 1000)\left(\frac{Pr_{ave}}{1 + 12.7\left(\frac{f}{8}\right)^{0.5}\left(Pr_{ave}^{\frac{2}{3}} - 1\right)}\right)\right]\left(\frac{Pr_{ave}}{Pr_p}\right)^{0.11}$$

$$\text{for} \quad 2300 < Re_D \quad (16)$$

with

$$f = (1.82\log(Re_D) - 1.64)^{-2} \quad (17)$$

The heat transfer from sun to the system $(\dot{Q}_{solar})$ can be calculated by:

$$\dot{Q}_{solar} = SA_{ap} F_R Col_s Col_r \quad (18)$$

The total mass flow rate of oil can be determined as follows:

$$\dot{m}_{oil} = Col_r \dot{m}_r \quad (19)$$

Also, the total area of collectors is:

$$A_{collector} = A_{ap} Col_s Col_r \quad (20)$$

3.2. Modeling of Rankine cycle

The power produced by the steam turbine is defined as:

$$\dot{W}_{st} = \dot{m}_{st}(h_5 - h_6) \quad (21)$$

The power consumed by solar and steam pumps can be calculated by Eqs. (22) and (23), respectively:

$$\dot{W}_{solar-pump} = \dot{m}_{oil}(h_1 - h_3) \quad (22)$$

$$\dot{W}_{steam-pump} = \dot{m}_{st}(h_4 - h_7) \quad (23)$$

Thus, thenet power for combined cycle is obtained by:

$$\dot{W}_{net} = \dot{W}_{st} - \dot{W}_{steam-pump} - \dot{W}_{solar-pump} \quad (24)$$

The thermal efficiency is:

$$\eta_{th} = \dot{W}_{net}/\dot{Q}_{solar} \quad (25)$$

The energy balance for evaporator and condenser can be written as follows, respectively:

$$\dot{Q}_{eva} = \dot{m}_2(h_2 - h_3) = \dot{m}_4(h_5 - h_4) \quad (26)$$

$$\dot{Q}_{cond} = \dot{m}_6(h_6 - h_7) = \dot{m}_8(h_9 - h_8) \quad (27)$$

3.3. Thermoeconomic analysis

In this section, thermoeconimc model is presented. The average cost of electricity $(c_w)$is obtained by:

$$c_w = \dot{Z}_{total}/\dot{W}_{net} \quad (28)$$

where

$$\dot{Z}_{total} = \sum_{k=1}^{nc} \dot{Z}_k \quad (29)$$

Here, nc is the number of components. Cost rate of each component $(\dot{Z}_k)$ is given by:

$$\dot{Z}_k = \frac{\varphi \times CRF \times PW}{\tau} \quad (30)$$

where capital recovery factor (CRF) is a function of interest rate (i) and lifetime of components (n).

$$CRF = \frac{i(i+1)^n}{(i+1)^n - 1} \quad (31)$$

The present worth is obtained as:

$$PW = TCI - SV(PWF) \quad (32)$$

where

$$PWF = \frac{1}{(i+1)^n} \quad (33)$$

and

$$SV = \mu\ (TCI) \quad (34)$$

whereμ is the salvage percentage. Table 2 presents the total capital investment (TCI) cost for each component. It shloud be mentioned that the surface area condenser and evaporator can be obtained by:

$$\dot{Q}_k = U_k A_k \Delta T_m \quad (35)$$

where, logarithmic mean temperature difference (ΔT_m) is calculated as:

$$\Delta T_m = \frac{(T_{h,in} - T_{c,out}) - (T_{h,out} - T_{c,in})}{\ln\left(\frac{T_{h,in} - T_{c,out}}{T_{h,out} - T_{c,in}}\right)} \quad (36)$$

Table. 2 Economic model for different components[13]

Component	Cost ($)
Solar collector	$TCI_{collector} = 240 A_{collector}$
Evaporator	$TCI_{eva} = (A_{eva}/0.093)^{0.78}$
Steam turbine	$TCI_{st} = 10^{[2.6259+1.4398\log(\dot{W}_{st})-0.1776(\log(\dot{W}_{st}))^2]}$
Pump	$TCI_{pump} = 10^{[3.3892+0.0536\log(\dot{W}_{pump})-0.1536(\log(\dot{W}_{pump}))^2]}$
Condenser	$TCI_{cond} = (A_{cond}/0.093)^{0.78}$

4. Results and discussion

In order to solve the governing equations, a code was extended in the Engineering Equation Solver (EES).The results are presented in four subsections.

4.1. Base conditions

Table 3 presents the thermodynamic properties of combined cycle at $G_b = 550\ W/m^2$, for $P_{ST} = 3972$ kPa and $T_{ST} = 318.3$ ℃. Also, Table 4shows the values of TCI ($) and $\dot{Z}$($/h) for each component. As it can be seen from the Table 4, the most expensive component is collector and the steam turbine is the second order. The cost of solar pump can be neglected. In the base conditions, the quality of outlet steam from the steam turbine is $x_6 =$

0.822 . The number of collector rows is obtained $Clo_r = 222$. The capital recovery factor is $CRF = 0.1339 (for\ i = 12\%\ and\ n = 20\ year)$. Other desirable values are obatined as $\dot{Z}_T = 683.905\ \$/h$, $\eta_{th} = 0.3014$ and $c_w = 3.42\ cent/kWh$ for $\dot{W}_{net} = 20\ kW$.

Tables. 3 The thermodynamic properties of combined cycle

State number	Fluid	ṁ(kg/s)	T(°C)	P(kPa)	h(kJ/kg)
1	Therminol-vp1	122.7	100	0.48	145.2
2	Therminol-vp1	122.7	333.33	423	633.2
3	Therminol-vp1	122.7	92.4	0.32	131.8
4	Water	23.57	45.95	3972	195.8
5	Steam	23.57	318.3	3972	3011
6	Two-phase steam	23.57	45.65	9.929	2158
7	Water	23.57	45.65	9.929	191.1
8	Water	1037.13	25	101.3	104.8
9	Water	1037.13	35	101.3	149.5

Table. 4 Economic values for each component

Component	TCI ($)	Ż($/h)
Solar collector	36102480	677.4
Evaporator	2560	0.048
Steam turbine	341125	6.4
Steam Pump	718.3	0.01348
Condenser	2236	0.04195
Solar Pump	93.97	0.0018

4.2. The effect of steam turbine inlet pressure

Fig. 3 presents the effect of steam turbine inlet pressure (P_{ST}) on the thermal efficiency (η_{th}) and the average cost of electricity (c_w). The figure shows that the thermal efficiency increases with increasing the steam turbine inlet pressure whereas the average cost of electricity decreases as the steam turbine inlet pressure increases. For example, η_{th} increases from 30.6% to 32% and c_w decreases from 3.09 to 2.96 cent/kWh (4.2% decreasing) when P_{ST} increases from 4500 to 7000 kPa. This is due to fact that with increasing the steam turbine inlet pressure, the number of collectors decreases. Therefore, the total cost of components decreases. For this figure, $G_b = 600\ W/m^2$.

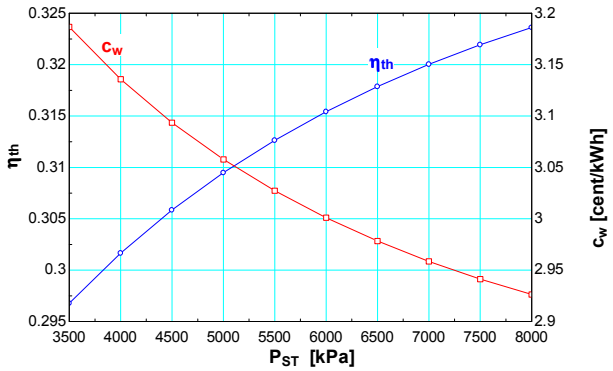

Fig. 3 The thermal efficiency (η_{th}) and the average cost of electricity (c_w) versus the steam turbine inlet pressure (P_{ST})

Fig. 4presents the effect of steam turbine inlet pressure(P_{ST}) on the number of collector rows (Col_r) for three different values of solar radiation(G_b).The figure indicates that the number of collector rows decreases with increasing the steam turbine inlet pressure. Also, it decreases when the value of solar radiation increases.For example, Col_r decreases from 230 to 192 (16.5% decreasing) when G_b increases from 500 to 600 W/m^2 at $P_{ST} = 6500\ kPa$because the amount of absorbed energy increases.

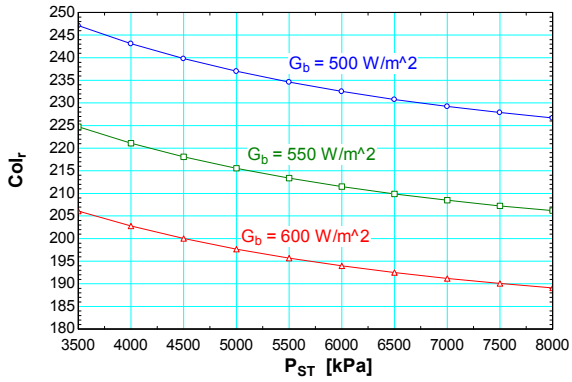

Fig. 4 The number of collector rows (Col_r) versus the steam turbine inlet pressure (P_{ST})

4.3. The effect of steam turbine inlet temperature

Fig. 5presents the effect of steam turbine inlet temperature (T_{ST}) on the thermal efficiency (η_{th}) and the average cost of electricity (c_w). The figure shows that the thermal efficiency increases with increasing the steam turbine inlet temperature whereas the average cost of electricity decreases as the steam turbine inlet temperature increases. For example, η_{th} increases from 29.87% to 30.14% and c_w decreases from 3.79 to 3.755 cent/kWh (1%

decreasing) when T_{ST} increases from 288 to 318 °C. This is due to fact that with increasing the steam turbine inlettemperature, the number of collectors decreases. Therefore, the total cost of components decreases. For this figure, $G_b = 500\ W/m^2$and $P_{ST} = 3972$ kPa.

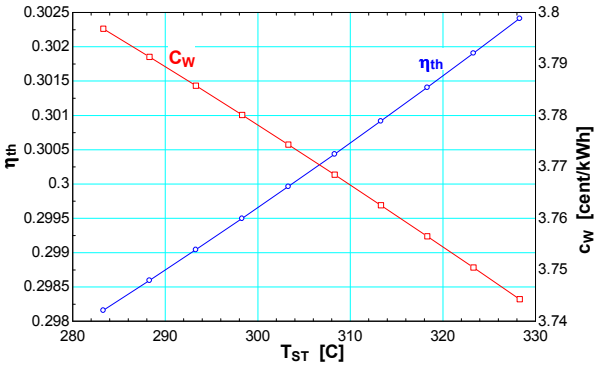

Fig. 5 The thermal efficiency (η_{th}) and the average cost of electricity (c_w) versus the steam turbine inlet temperature (T_{ST})

Fig. 6presents the effect of steam turbine inlet temperature (T_{ST})on the number of collector rows (Col_r) for three different values of solar radiation(G_b).The figure indicates that the number of collector rows decreases with increasing the steam turbine inlet temperature. Also, it decreases when the value of solar radiation increases. For example, Col_r decreases from 245 to 205 (16.3% decreasing) when G_b increases from 500 to 600 W/m^2 at $T_{ST} = 298$ °C because the amount of absorbed energy increases.

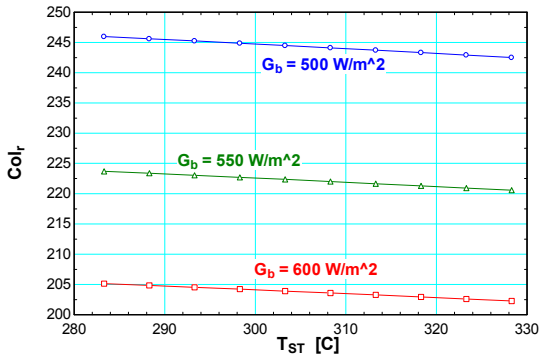

Fig. 6 The number of collector rows (Col_r) versus the steam turbine inlettemperature (T_{ST})

Fig. 7 illustrates variations of the steam turbine inlet temperature (T_{ST}) and the total area of collectors $(A_{collector})$versuspinch point temperature difference(ΔT_{PP}). The figure shows that thesteam turbine inlettemperature decreases whereas the total area of collectors increases as the pinch point temperature difference gose up.

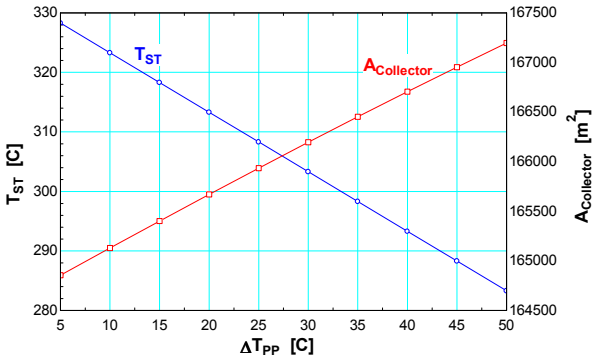

Fig. 7 The steam turbine inlet temperature (T_{ST}) and the total area of collectors $(A_{collector})$ versus pinch point temperature difference (ΔT_{PP})

4.4. The effect of interest rate and lifetime

Fig. 8 shows variations of the average cost of electricity (c_w) versus interest rate (i) for three values of lifetime (n). As shown, the average cost of electricity increases when the interest rate increases for each value of lifetime. On the other hand, the average cost of electricity decreases when the lifetime increases for each value of interest rate. This behavior is acceptable according to Eqs. (28) –(31). For example, c_w increases from 2.8 to 5 cent/kWh (78.6% increasing) when i increases from 10% to 19% for $n = 25$.

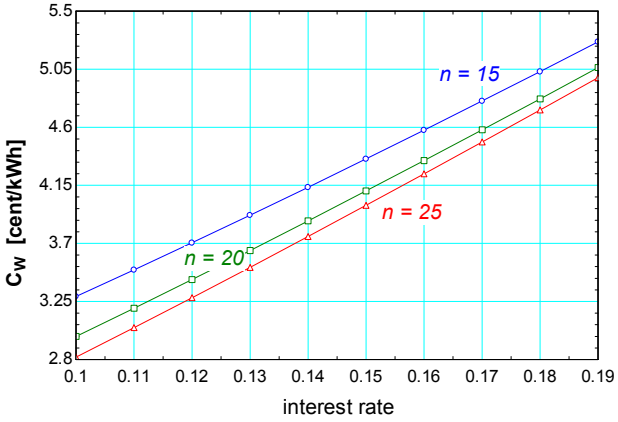

Fig. 8 The average cost of electricity (c_w) versus the interest rate(i)for different lifetime(n)

5. Conclusions

In this paper, thermoeconomic analysis was performed for a steam Rankine cycle with PTSC. The model of PTSC is performed by a extended code in EES. The main results

are as follows:

- The average cost of electricity decreases as the steam turbine inlet pressure increases. For example, c_w decreases 4.2% when P_{ST} increases from 4500 to 7000 kPa.
- The number of collector rows decreases with increasing the steam turbine inlet pressure.
- The average cost of electricity decreases as the steam turbine inlet temperature increases.
- The number of collector rows Col_r decreases 16.3% when G_b increases from 500 to 600 W/m^2.
- The average cost of electricity increases when the interest rate increases whereas it decreases when the lifetime increases.

References

[1] E. Zarza, ME. Rojas, L. González, JM. Caballero, F. Rueda,"INDITEP: the first precommercial DSG solar power plant", Sol Energy. Vol. 80:1270-6,2006.

[2] B. Zheng,Y.W. Weng,"A combined power and ejector refrigerationcycle for low temperature heat sources", Solar Energy, Vol. 84, No.5:784–791, 2010.

[3] F. A. Al-Sulaiman, Ibrahim Dincer, Feridun Hamdullahpur, "Exergy modeling of a new solar driven trigeneration system" , Solar Energy, Vol. 85: 2228–2243, 2011.

[4] Soteris A. Kalogirou," A detailed thermal model of a parabolic trough collector receiver", Energy, Vol. 48: 298-306, 2012.

[5] I. Niknia,M. Yaghoubi, "Transient simulation for developing a combined solarthermal power plant", Appl. Therm. Eng. , Vol.37:196-200, 2012.

[6] Fahad A. Al-Sulaiman," Energy and sizing analyses of parabolic trough solar collectorintegrated with steam and binary vapor cycles", Energy, Vol. 58: 561-570, 2013.

[7] Fahad A. Al-Sulaiman," Exergy analysis of parabolic trough solar collectors integratedwith combined steam and organic Rankine cycles", Energy Conversion and Management , Vol.77: 441–449, 2014

[8] Nasir MT, Kim KC., "Working fluids selection and parametric optimization of an OrganicRankine Cycle coupled Vapor Compression Cycle (ORC-VCC) for airconditioning using low grade heat", Energy Build., Vol. 129:378–95, 2016.

[9] Halimeh Rashidi, Jamshid Khorshidi," Exergoeconomic analysis and optimization of a solar based multigeneration system using multiobjective differential evolution algorithm", Journal of Cleaner Production, Vol. 170 : 978-990, 2018.

[10] S. Khanmohammadi, M. Saadat-Targhi, A. Al-Rashed , M. Afrand, "Thermodynamic andeconomic analyses and multi-objective optimization of harvesting waste heat from abiomass gasifier integrated system by thermoelectric generator", Energy Convers. Manage. Vol. 195:1022–34, 2019.

[11] Saman Khalilzadeh, Alireza Hossein Nezhad, Faramarz Sarhaddi, "Reducing the power consumption of cascade refrigeration cycle by a newintegrated system using solar energy", Energy Conversion and Management, Vol. 200 , 2019.

[12] Parabolic Trough Reflector for Solar Thermal System. Available online:http://www.alternative-energytutorials.com/solar-hot-water/parabolic-trough-reflector.html(accessedon 29 December 2018).

[13] A. Abdollahpour A, R. Ghasempour , A. Kasaeian , MH. Ahmadi, "Exergoeconomic analysisand optimization of a transcritical CO2 power cycle driven by solar energy based onnanofluid with liquefied natural gas as its heat sink", J Therm Anal Calorim, Vol. 139:1–23, 2019.